

# Simulation of Emergent Rippling on Growing Thin-Shells

Danny Huang  
University of Saskatchewan  
danny.huang@usask.ca

Ian Stavness  
University of Saskatchewan  
ian.stavness@usask.ca

## CCS CONCEPTS

• **Computing methodologies** → **Physical simulation**; *Interactive simulation*;

## KEYWORDS

Simulation, Growth, Finite Element Method, Shells, Tissue, Leaf

### ACM Reference Format:

Danny Huang and Ian Stavness. 2018. Simulation of Emergent Rippling on Growing Thin-Shells. In *Proceedings of SIGGRAPH '18 Posters*. ACM, New York, NY, USA, 2 pages. <https://doi.org/10.1145/3230744.3230790>

## 1 INTRODUCTION

Many thin tissues, such as leaves and flower petals, exhibit rippling and buckling patterns along their edge as they grow (Figure 1). Experiments with plastic materials have replicated the rippling patterns found in nature and shown that such patterns exhibit a fractal quality of ripples upon ripples — a so called “buckling cascade” [Eran et al. 2004]. Such patterns are influenced by many physical mechanisms, including stress forces, physical properties of materials (e.g., stiffness), and space constraints [Prusinkiewicz and Barbier de Reuille 2010]. Physics-based computer animation that produces emergent rippling patterns on thin surface can improve the realism of virtual flowers and leaves, and also help to explain which physical mechanisms are most important for controlling the morphology of tissues with buckling cascades.

Simulating the mechanics of thin, growing biological tissues is a challenging task as it requires the integration of many physics-simulation components. In particular, growing tissue models require the simulation of thin structures, elastic deformations, inelastic “growth” deformations, non-homogeneous materials, morphogen diffusion, collision detection, remeshing, and other components. The majority of thin structure simulation methods in computer graphics only consider elastic deformations and isotropic materials.

Along with the difficulty of incorporating all the components required for growth, there is a limitation in the current experiments where the thin structure of growing tissue are modeled using either spring-masses [Prusinkiewicz and Barbier de Reuille 2010] or solid finite elements [Kennaway et al. 2011]. In a spring-mass model, it is generally less stable, does not accurately represent continuum mechanics like finite-element analysis, and does not intrinsically account for bending resistance in a model with a single layer of springs. While solid finite elements can be used instead



**Figure 1: Natural occurrences of tissue rippling and our simulated model. The *Brassica oleracea* (kale) leaf on the left and *Lagerstroemia* (crape myrtle) flower in the middle, exhibit rippling along their edge. The right shows our simulation of rippling using prestressed thin-shell finite elements.**

of spring-masses to overcome these shortcomings, these volumetric elements have their own limitations when representing thin structures. While a thin structure can be constructed using a single layer of volumetric elements with a small height each, the width and length of each element also needs to be small to maintain well-conditioned elements, reducing the risk of encountering highly distorted or inverted elements. However, many of these smaller elements would be needed to fill the thin structure which greatly increases the computational complexity of the model.

We propose an interactive tissue growth simulation method that currently integrates thin-shell finite elements with elastic and inelastic deformation to represent the elasticity and permanent deformation of growing tissue. We show that our growing thin-shell simulations can produce spontaneous emergent buckling cascades. We compare our growing thin-shell formulation to matched spring-mass and solid finite element models, and also illustrate how tissue thickness alters the pattern of tissue rippling.

## 2 METHOD

To demonstrate and compare our growth simulation method, we simulated four variations of a previously-published tissue rippling model of a kale leaf [Prusinkiewicz and Barbier de Reuille 2010]. In particular, the simulation begins with four planar tissue side-by-side, composed of spring-masses, coarse solids, fine solids, and thin-shells respectively. From there, all four variations follow the same procedure to generate rippling. All simulations were performed in the Artisynt 3D biomechanical modelling toolkit [Lloyd et al. 2012] that readily offers construction, simulation, and interaction of spring-mass and finite-element models.

The spring-mass variation of the tissue rippling model was designed to closely match the model’s original implementation [Prusinkiewicz and Barbier de Reuille 2010]. In both implementations, the tissue is composed of spring-mass triangles. At regular intervals, an extra row of tissue was appended on top. Each row of tissue carries some prestress that causes expansion of itself along the tissue plane. This prestress is simulated by relaxing the compressed springs. Unlike the original implementation, our tissues

Permission to make digital or hard copies of part or all of this work for personal or classroom use is granted without fee provided that copies are not made or distributed for profit or commercial advantage and that copies bear this notice and the full citation on the first page. Copyrights for third-party components of this work must be honored. For all other uses, contact the owner/author(s).

SIGGRAPH '18 Posters, August 12–16, 2018, Vancouver, BC, Canada

© 2018 Copyright held by the owner/author(s).

ACM ISBN 978-1-4503-5817-0/18/08.

<https://doi.org/10.1145/3230744.3230790>

will not be manually perturbed to seed buckling. Instead, when enough additional tissue is grown, it is expected that residual stress and numerical error will have accumulated enough in the tissue for buckling to occur automatically.

In the coarse solid variation, the implementation is the same as the spring-mass variation except each spring-mass triangle is replaced with a 6-node 3D wedge solid finite element. Instead of relaxing compressed springs to simulate prestress, each solid element has an inelastic deformation gradient multiplied to its usual elastic deformation gradient [Cyron et al. 2017]. This way, prestress is simulated as permanent deformation across the entire element instead of just its edges. To permit large deformations, linear corotated elastic material was used. The fine solid variation is identical to its coarse counterpart except the tissue is composed using smaller elements. Specifically, the fine solid variation had 2x more elements.

The thin-shell tissue is the same as the coarse solid tissue except each element is a 3-node triangular thin-shell finite element. The thin-shell finite element was implemented based on the degenerated concept where a 6-node wedge is represented and rendered as a 3-node triangle [Betsch et al. 1996]. Specifically, only the triangular mid-surface, residing between the thickness of the wedge, is represented. Each mid-surface node has an intersecting *director* vector to represent the thickness at that node. The virtual thickness approach simplifies computation and is more stable because traverse shear deformation is ignored.

### 3 RESULTS AND DISCUSSION

Among the four different models, we compared their resultant rippling morphologies and stability. Initially for the spring-mass model, it was unable to generate any buckling on its own. This is likely explained by the larger particle masses used for stability, allowing more prestress energy to be accommodated along the plane. To at least provide comparable results, we seeded buckling by perturbing it during growth, which triggered a rippling cascade pattern with sharp curvatures (Figure 2.A). We believe that the unnatural sharpness is due to its lack of bending resistance and weaker representation of continuum mechanics. For the coarse solid model (Figure 2.B), it encountered inverted element errors but was stable enough to spontaneously produce ripples with smooth curvatures. The fine solid model counterpart (Figure 2.C) and thin-shell model (Figure 2.D) both simulated stably and produced more noticeable second-order rippling.

When growth finished, we averaged the computation time of the subsequent 100 time steps. Specifically, the spring-mass (3068 triangles), solid (3068 elements), fine solid (6137 elements), and thin-shell (3068 elements) models respectively required an average of 43 ms, 67 ms, 124 ms, and 83 ms per time step.

We also analyzed the correlation between thin-shell thickness and buckling wavelength. We observed that increasing the thickness generated larger wavelengths (Figure 3), which is consistent with experiments performed on plastic materials [Eran et al. 2004].

To conclude, this paper demonstrates one application of simulating growth using deformable thin-shells. As future work, we plan on integrating more simulation components, such as non-homogeneous materials, diffusion of morphogens, and handling self-collisions to offer improved methods for simulating tissue growth.

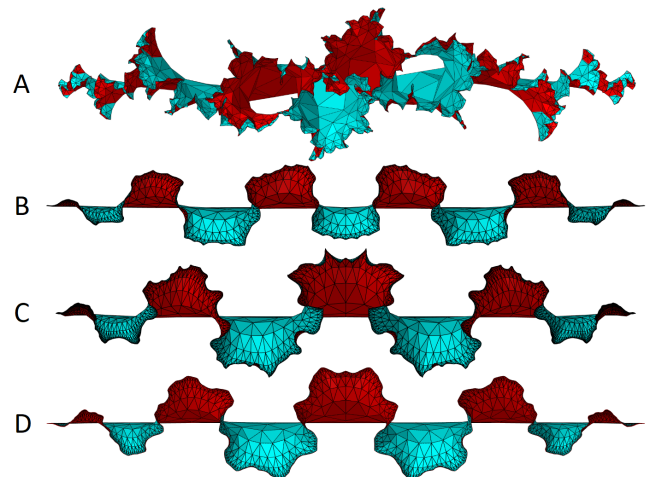


**Figure 2: Top-down view of the rippling patterns produced by different models. The spring-mass model (A), with needed perturbation to trigger buckling, produced sharp rippling cascades. The solid model (B) encountered inverted element errors but was stable enough to produce smooth ripples spontaneously. The fine solid model (C) with 2x more elements, and the thin-shell model (D) with virtual thickness, avoided the errors and produced more noticeable second-order rippling.**

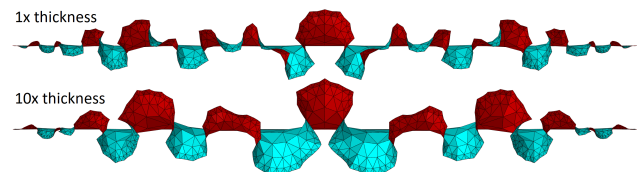


**Figure 3: Simulations illustrating the relationship between thin-shell thickness and buckling wavelength. By increasing the thickness, the wavelengths increases as well.**

### ACKNOWLEDGMENTS

We thank Przemyslaw Prusinkiewicz, Mikolaj Cieslak, and John Lloyd for their helpful discussions on this work.

This research was undertaken thanks in part to funding from the Canada First Research Excellence Fund.

### REFERENCES

- P Betsch, F Gruttmann, and E Stein. 1996. A 4-node finite shell element for the implementation of general hyperelastic 3D-elasticity at finite strains. *Computer Methods in Applied Mechanics and Engineering* 130, 1-2 (1996), 57–79.
- CJ Cyron, JS Wilson, and JD Humphrey. 2017. Constitutive formulations for soft tissue growth and remodeling. In *Biomechanics of Living Organs*. Elsevier, 79–100.
- Sharon Eran, Michael Marder, and Harry L Swinney. 2004. Leaves, flowers and garbage bags: making waves. *American Scientist* 92, 3 (2004), 254.
- Richard Kennaway, Enrico Coen, Amelia Green, and Andrew Bangham. 2011. Generation of diverse biological forms through combinatorial interactions between tissue polarity and growth. *PLoS computational biology* 7, 6 (2011), e1002071.
- JE Lloyd, I Stavness, and S Fels. 2012. ArtiSynth: A fast interactive biomechanical modeling toolkit combining multibody and finite element simulation. In *Soft Tissue Biomech Modeling for Computer Assisted Surgery*. Springer, 355–394.
- Przemyslaw Prusinkiewicz and Pierre Barbier de Reuille. 2010. Constraints of space in plant development. *Journal of experimental botany* 61, 8 (2010), 2117–2129.